Erp29 Attenuates Cigarette Smoke Extract–Induced Endoplasmic Reticulum Stress and Mitigates Tight Junction Damage in Retinal Pigment Epithelial Cells

Chuangxin Huang,[1–3] Joshua J. Wang,[2–4] Guangjun Jing,[4] Junhua Li,[2,3] Chenjin Jin,[1] Qiang Yu,[1] Marek W. Falkowski,[2] and Sarah X. Zhang[2,3]

[1]State Key Laboratory of Ophthalmology, Zhongshan Ophthalmic Center, Sun Yat-sen University, Guangzhou, China
[2]Departments of Ophthalmology and Biochemistry, Ross Eye Institute, University at Buffalo, State University of New York, Buffalo, New York, United States
[3]SUNY Eye Institute, State University of New York, Buffalo, New York, United States
[4]Department of Medicine, University of Oklahoma Health Sciences Center, Oklahoma City, Oklahoma, United States

Correspondence: Sarah X. Zhang, Departments of Ophthalmology and Biochemistry, University at Buffalo, State University of New York, 3435 Main Street, Buffalo, NY 14214, USA; xzhang38@buffalo.edu.

CH and JJW contributed equally to the work presented here and should therefore be regarded as equivalent authors.

Submitted: March 3, 2015
Accepted: August 21, 2015

Citation: Huang C, Wang JJ, Jing G, et al. ERp29 attenuates cigarette smoke extract–induced endoplasmic reticulum stress and mitigates tight junction damage in retinal pigment epithelial cells. *Invest Ophthalmol Vis Sci*. 2015;56:6196–6207. DOI:10.1167/iovs.15-16795

Purpose. Endoplasmic reticulum protein 29 (ERp29) is a novel chaperone that was recently found decreased in human retinas with AMD. Herein, we examined the effect of ERp29 on cigarette smoke–induced RPE apoptosis and tight junction disruption.

Methods. Cultured human RPE (HRPE) cells (ARPE-19) or mouse RPE eyecup explants were exposed to cigarette smoke extract (CSE) for short (up to 24 hours) or long (up to 3 weeks) periods. Expression of ERp29 was up- and downregulated by adenovirus and siRNA, respectively. Endoplasmic reticulum stress markers, apoptosis, and cell death, the expression and distribution of tight junction protein ZO-1, transepithelial electrical resistance (TEER), and F-actin expression were examined.

Results. Endoplasmic reticulum protein 29 was significantly increased by short-term exposure to CSE in ARPE-19 cells or eyecup explants but was reduced after 3-week exposure. Overexpression of ERp29 increased the levels of GRP78, $p58^{IPK}$, and Nrf-2, while reducing p-eIF2α and C/EBP homologous protein (CHOP), and protected RPE cells from CSE-induced apoptosis. In contrast, knockdown of ERp29 decreased the levels of $p58^{IPK}$ and Nrf2, but increased p-eIF2α and CHOP and exacerbated CSE-triggered cell death. In addition, overexpression of ERp29 attenuated CSE-induced reduction in ZO-1 and enhanced the RPE barrier function, as measured by TEER. Knockdown of ERp29 decreased the level of ZO-1 protein. These effects were associated with changes in the expression of cytoskeleton F-actin.

Conclusions. Endoplasmic reticulum protein 29 attenuates CSE-induced ER stress and enhances cell viability and barrier integrity of RPE cells, and therefore may act as a protective mechanism for RPE survival and activity.

Keywords: RPE, apoptosis, tight junction, ERp29

Endoplasmic reticulum protein 29 (ERp29) is an endoplasmic reticulum (ER) luminal protein ubiquitously expressed among tissues and cell types.[1–5] Endoplasmic reticulum protein 29 is inducible under cellular stress, such as thapsigargin- or tunicamycin-induced ER stress in rat hepatoma cells[2] or naloxone-induced ER stress in PC12 cells.[6] Structural studies have revealed that ERp29 contains a N-terminal thioredoxin domain that resembles protein disulfide isomerase (PDI),[7] and may play a role in protein folding. Furthermore, ERp29 has been shown to interact with and enhance the function of other ER chaperones, such as GRP94, GRP78, ERp72, and calnexin.[8] Additionally, ERp29 upregulates the chaperones involved in stress response pathways, such as $p58^{IPK}$, p-eIF2α, p38, or Hsp27, promoting cell survival under stress conditions.[2,8–11] Overexpression of ERp29 attenuates doxorubicin-induced cell death of breast cancer cells,[12] while silencing ERp29 expression increases the sensitivity of cancer cells to apoptosis through regulation of Hsp27.[13] These findings have implied an important role of ERp29 in the regulation of cell survival and apoptosis. In addition, a recent study reported that ERp29 suppresses the epithelial-mesenchymal transition (EMT) of cancer cells, indicating a potential effect of ERp29 on modulation of epithelial cell integrity.[14]

Age-related macular degeneration (AMD) is the leading cause of blindness in elderly people in developed countries. Clinically, AMD can be divided into two types in the late stage: (1) neovascular AMD, which is characterized by choroidal neovascularization (CNV) formation, and (2) geographic atrophy (GA), which is characterized by the loss of the choriocapillaries and overlying RPE.[15,16] The RPE consists of a monolayer of cuboidal pigmented epithelial cells, which play a critical role in supporting photoreceptor cell survival, outer segment renewal, and visual signal transduction. These cells also form the outer blood–retinal barrier (BRB) to ensure the homeostatic environment of the neural retina. Disturbances in the RPE function and structure are considered a central event in the pathogenesis of AMD.[17] Furthermore, disruption of the RPE integrity resulting in loss of epithelial cell property and EMT are

believed to contribute to CNV formation.[18] Interestingly, a recent study shows that the expression of ERp29 is decreased in the retina and RPE of human macula with AMD[19]; however, the precise role of ERp29 in the development of AMD and RPE injury has not been studied.

Among the risk factors identified to influence the development and progression of AMD, cigarette smoke is the most significant environmental factor.[20–23] In fact, cigarette smoke–induced RPE damage has been widely used in AMD-related studies.[24,25] Recent works by our group and others have demonstrated that exposure to cigarette smoke or cigarette smoke extract (CSE) induces ER stress and apoptosis in mouse RPE or cultured human RPE (HRPE) cells.[26–28] In the present study, we investigate the role of ERp29 in CSE-induced RPE injury. We hypothesize that CSE upregulation of ERp29 acts as a protective mechanism that promotes RPE cell survival through regulation of other ER chaperones and antioxidant factors, thereby reducing ER and oxidative stress. Additionally, we evaluate the potential effect of ERp29 on the regulation of tight junction formation and cell barrier integrity in CSE-challenged ARPE-19 cells.

Materials and Methods

CSE Preparation

As previously described,[29,30] CSE (dissolved in DMSO, 40 mg/mL total particular matter, nicotine content 6%) was purchased from Murty Pharmaceuticals (Lexington, KY, USA) and was kept at −20°C. Before each treatment, CSE was freshly prepared into working solution with desired concentrations.

Cell Culture

Human RPE cells (ARPE-19; American Type Culture Collection [ATCC], Manassas, VA, USA) were cultured as previously described.[30] Briefly, ARPE-19 cells were cultured with Dulbecco's modified Eagle's medium (DMEM)/F12 medium containing 10% fetal bovine serum (FBS) and a 1% antibiotic/antimycotic suspension. For general experiments, ARPE-19 cells were cultured to 70% confluence, then starved overnight with low-serum (1% FBS) DMEM/F12 medium, followed by desired treatment. For experiments involving RPE tight junctions, ARPE-19 cells were cultured to 100% confluence and maintained with serum-free DMEM for 2 to 3 weeks before CSE treatment.

Preparation and Culture of RPE Eyecup Explants

Retinal pigment epithelial eyecup explants containing sclera, choroid, and RPE were prepared and cultured according to a previously published protocol.[31] Briefly, dissected mouse eyes were placed in ice-cold PBS. The anterior segments and the retinas were gently removed. The eyecups were cultured in DMEM/F-12 containing 10% FBS and a 1% antibiotic/antimycotic for 24 hours, and then exposed to CSE (320 μg/mL) for an additional 24 hours. Proteins were extracted and subjected to Western blot analysis.

Construction and Transduction of Adenoviruses

Recombinant adenovirus expressing human ERp29 was constructed using the AdEasy system (Agilent Technologies, Santa Clara, CA, USA).[32] Briefly, full-length human ERp29 gene was cloned using primers: forward primer AAACTCGAGGCCA CATGGCTGCCGCTGTGCCCCGC; and reverse primer CCCAAGCTTTTACAGCTCCTCTTTCTCGGC, and inserted into the KpnI-XhoI sites of the vector pShuttle-CMV. The resultant plasmid was cotransformed with pAdEasy-1 adenoviral vector into BJ5183 *Escherichia coli* competent cells by electroporation. The recombinant adenoviral plasmids were then transfected into the packing cell line 293AD to generate recombinant adenoviruses. Transduction of adenovirus expressing ERp29 to ARPE-19 cells was performed as previously described.[33] Adenovirus expressing green fluorescent protein (GFP) was used as the control. After 24 hours of transduction, cells were starved with 1% FBS DMEM/F12 medium, followed by CSE treatment.

Small-Interfering RNAs (siRNAs)

ARPE-19 cells were transfected with siRNA against human ERp29 (Santa Cruz Biotechnology, Inc., Santa Cruz, CA, USA) using Lipofectamine 2000 (Invitrogen, Carlsbad, CA, USA) following the manufacturer's instructions, as previously described.[34] A control siRNA (Santa Cruz Biotechnology, Inc.) which does not recognize any known homology to mammalian genes was set as the negative control. The knockdown efficiency was detected by determining the protein level using Western blot analysis.

Western Blot Analysis

Cells or eyecup explants were harvested using lysis buffer (Santa Cruz Biotechnology, Inc.) containing 150 mM NaCl, 1% Igepal, 50 mM Tris, 1 mM EDTA, and 10% protease inhibitor mixture. Protein quantification was performed using the bicinchoninic acid (BCA) method (Thermo Scientific, Rockford, IL, USA). Ten micrograms of total cellular or eyecup protein was fractionated on 10% SDS-PAGE gels, electroblotted onto an immunoblot polyvinylidene difluoride membrane (Bio-Rad, Hercules, CA, USA), and blocked with 5% nonfat dry milk TBST buffer for 1 hour. After blocking, the membranes were blotted overnight at 4°C with the following primary antibodies: anti-ERp29 (1:1000; Abcam, Cambridge, MA, USA); anti-GRP78 (1:1000; Abcam); anti-p-eIF2α (1:1000; Cell Signaling, Danvers, MA, USA); anti–/EBP homologous protein (CHOP; 1:1000; Cell Signaling); anti-Nrf2 (1:1000; Santa Cruz Biotechnologies, Inc.); anti-p58^{IPK} (1:1000; Cell Signaling); anti–cleaved caspase-3 (1:500; Cell Signaling); anti-PARP (1:2000; Cell Signaling); and anti ZO-1 (1:1000; Cell Signaling). After incubation with HRP-conjugated secondary antibodies, the membranes were developed with chemiluminescence substrate (Thermo Fisher Scientific, Waltham, MA, USA) using a Chemi Doc MP Imaging System (Bio-Rad). The membranes were reblotted with anti–β-actin (1:20,000; Abcam) for normalization. The bands were semiquantified by densitometry using Bio-Rad imaging software.

TUNEL Assay

According to the manufacturer's protocol and the existing literature, the TUNEL assay was performed using the In Situ Cell Death Detection TMR Red Kit (Roche Diagnostics Corp., Indianapolis, IN, USA), as previously described.[35] Briefly, cells were fixed with 4% paraformaldehyde (PFA) for 1 hour, permeabilized in 0.1% citrate buffer containing 0.1% Triton X-100 for 2 minutes on ice, then incubated in a TUNEL reaction mix containing nucleotides and terminal deoxynucleotidyl transferase (TdT) at 37°C for 1 hour. Incubation without the TdT enzyme served as a negative control. After incubation, the coverslips were mounted onto slices using mounting medium containing 4′-6-diamidino-2-phenylindole (DAPI; Vector Labo-

Investigative Ophthalmology & Visual Science

ratories, Burlingame, CA, USA), and observed under a fluorescence microscope.

In Situ Trypan Blue Staining

Cultured ARPE-19 cells were stained in situ with 0.04% trypan blue in DMEM/F12 media for 15 minutes.[36] The number of trypan blue–stained and total cells was counted under a microscope.

Immunocytochemisty

ARPE-19 cells cultured on coverslips were fixed with 4% paraformaldehyde (PFA) for 20 minutes, blocked, and permeabilized in 5% BSA 0.3% Triton-X 100 PBS buffer. After washing with PBS three times, cells were incubated at 4°C overnight with the following primary antibodies: anti-ERp29 (1:500; Abcam); anti–ZO-1 (1:400; Zymed, South San Francisco, CA, USA), anti-pan-cadherin (1:100; Thermo Scientific), and anti–β-catenin (1:30; Thermo Scientific). Antibodies were visualized using 488- or Cy3-conjugated secondary antibody and observed under a fluorescence microscope. For phalloidin staining to detect F-actin, cells were incubated with phalloidin staining solution (1:200; Invitrogen) at 20°C for 30 minutes.

Tight Junction Morphologic Grading

The tight junction morphologic grading was modified based on a previously described study.[37] After ZO-1 staining, the slices were observed under a fluorescence microscope and at least five images on a ×10 microscopic field were captured for each slice. All the images were separated into 25 small grids using ImageJ software (http://imagej.nih.gov/ij/; provided in the public domain by the National Institutes of Health, Bethesda, MD, USA). The different manifestations of tight junctions in each small grid were graded as one of four levels: "smooth"; "complete"; "broken"; and "disappeared." "Smooth" indicated that greater than or equal to 70% of cells presented complete, tight, and smooth tight junctions in one grid, suggesting a very good tight junction. "Complete" indicated greater than or equal to 70% of cells presented complete, but rough tight junctions in one grid, suggesting a good tight junction. "Broken" indicated greater than or equal to 70% of cells presented broken, but visible tight junctions in one grid, suggesting a mildly damaged tight junction. "Disappeared" indicated greater than or equal to 70% of cells lost tight junctions in one grid, suggesting a severely damaged tight junction. The total grid number of each grade in each picture was counted, and the total "smooth" or "disappeared" grid numbers were analyzed to compare the differences between the ERp29 and GFP groups.

Transepithelial Electrical Resistance

Transepithelial electrical resistance (TEER) was measured with an EVOMX voltohmmeter (World Precision Instruments, Sarasota, FL, USA). The substrate for which the resistance of cell-free collagen-coated Transwell inserts from each experimental point is presented as absolute values (Ohm × cm^2).

Statistical Analysis

The quantitative data were expressed as the mean ± SD. Statistical analyses were performed using unpaired Student's *t*-test when comparing two groups and 1-way ANOVA with Bonferroni's multiple comparison test for three groups or more. Statistical differences were considered significant at a P value less than 0.05.

Results

CSE Alters the Expression of Erp29 in RPE Cells

Previously, we showed that exposure of ARPE-19 cells to 320 μg/mL CSE for 6 to 24 hours sequentially induced ER stress and apoptosis.[32] We determined whether or not induction of ER stress by CSE affects ERp29 expression. As shown in Figure 1A, CSE exposure induced a time-dependent increase in ERp29 expression in ARPE-19 cells. Immunostaining confirmed this result and revealed a paranuclear localization of ERp29 in both unstimulated and CSE-treated cells (Fig. 1B). To further confirm the induction of CSE in the RPE, mouse eyecup explants were exposed to CSE for 24 hours. Western blot analysis showed that the level of ERp29 was significantly increased (>1.5-fold) in CSE-stressed RPE explants, suggesting that CSE is a potent inducer of ERp29 in the RPE (Fig. 1C). To determine how chronic CSE treatment affects ERp29 expression, confluent ARPE-19 cells were cultured with 10 to 40 μg/mL CSE in serum-free medium for 10 days or 3 weeks. Endoplasmic reticulum protein 29 expression was found unchanged after CSE treatment for 10 days but dose-dependently decreased after CSE treatment for 3 weeks. These changes are accompanied by reduced levels of ZO-1 (a tight junction protein), GRP78, and GRP94 (ER chaperones; Figs. 1D, 1E).

Overexpression of Erp29 Attenuates CSE-Induced ER Stress in ARPE-19 Cells

Studies have shown that ERp29 can modulate the levels of ER chaperones and other ER stress–inducible proteins, such as $p58^{IPK}$, thereby reducing ER stress.[9] To determine if ERp29 regulates ER stress in ARPE-19 cells, we overexpressed ERp29 using adenovirus. Cells transduced with Ad-GFP were used as a control. After adenoviral transduction, cells were exposed to 320 μg/mL CSE for 6 or 24 hours, and Western blot analysis was performed to examine the expression of target proteins. Our results showed that ERp29 significantly increased the levels of GRP78 and $p58^{IPK}$, but decreased CSE-induced expression of p-eIF2α and CHOP, a major mediator of ER stress-related apoptosis (Fig. 2). Interestingly, expression of Nrf2, a central regulator of phase II detoxification enzymes and antioxidant proteins, was also increased by ERp29. This result suggests that overexpression of ERp29 attenuates CSE-induced ER stress, which may function by promoting protein folding, increasing expression of GRP78 and $p58^{IPK}$, and modulating the redox status by enhancing Nrf2.

Overexpression of Erp29 Suppresses CSE-Induced Apoptosis and Promoted Cell Survival

To further examine whether overexpression of ERp29 affects survival of RPE cells, adenoviral-transduced ARPE-19 cells were exposed to 320 μg/mL CSE for 24 hours. Apoptosis was examined by Western blot analysis to measure the activation of caspase-3, and the TUNEL assay was used to detect apoptotic cells. Cigarette smoke extract treatment significantly increased the level of cleaved caspase-3, indicating activation of this enzyme, which was almost completely blocked by ERp29 (Fig. 3A). The TUNEL assay revealed fewer apoptotic cells in the ERp29 group after CSE treatment when compared with the control group (Fig. 3B). Furthermore, trypan blue staining confirmed that CSE significantly increased the number of dead

Investigative Ophthalmology & Visual Science

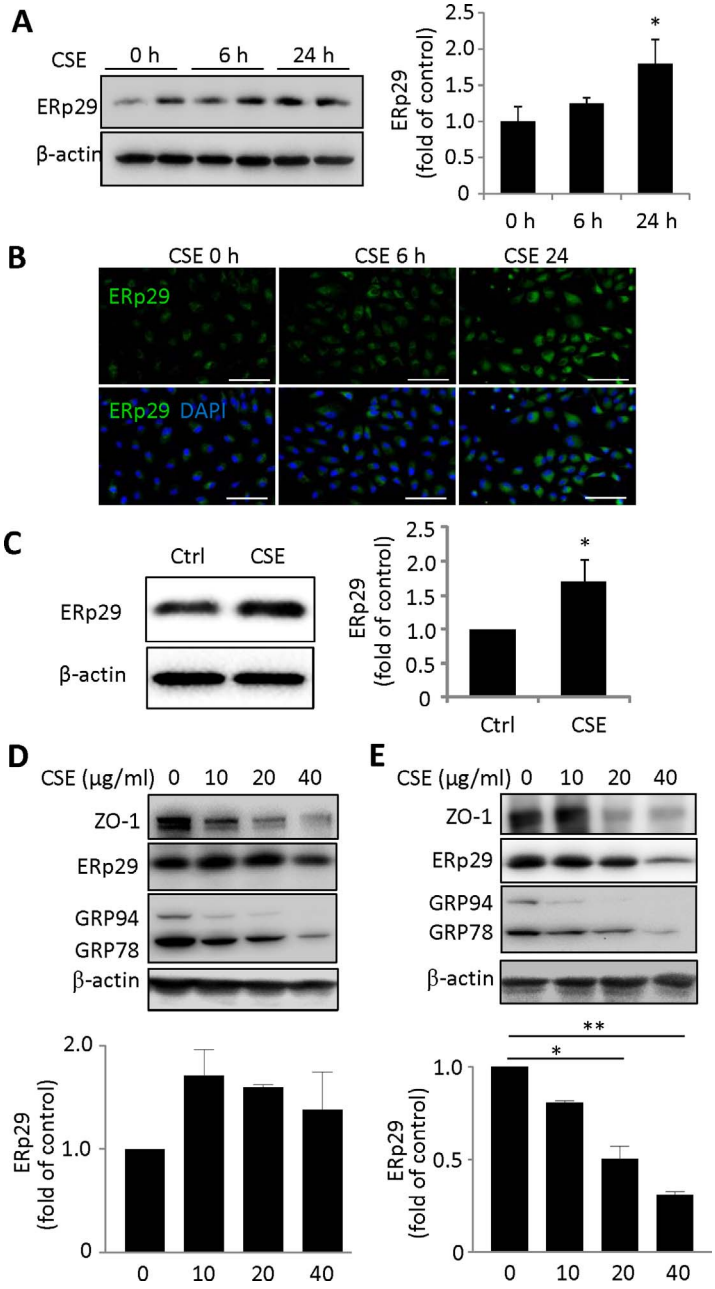

Figure 1. Exposure to CSE alters the expression of ERp29 in HRPE cells. (**A**) ARPE-19 cells were exposed to CSE at a dose of 320 μg/mL for 6 or 24 hours. *Left*: Western blot results of ERp29. *Right*: ERp29 level quantified by densitometry and normalized with β-actin. (**B**) Immunofluorescence staining of ERp29 after exposure to CSE for 6 or 24 hours. *Scale bars*: 100 μm. (**C**) ERp29 expression of mouse eyecup explants after exposure to CSE (320 μg/mL) for 24 hours. *Left*: Western blot result of ERp29. *Right*: ERp29 level quantified by densitometry and normalized with β-actin. (**D**, **E**) ARPE-19 cells were exposed to 10 to 40 μg/mL CSE for 10 days (**D**) and 3 weeks (**E**). *Lower*: ERp29 levels quantified by densitometry and normalized with β-actin. Data are expressed as the mean ± SD from three independent experiments in (**A**–**C**, **E**) and two independent experiments in (**D**). $^{*}P < 0.05$ versus control, $^{**}P < 0.01$.

cells in the control group, and to a lesser extent in the ERp29 group (Fig. 3C).

Knockdown of Erp29 Expression Exacerbates CSE-Induced ER Stress and Apoptosis in ARPE-19 Cells

To determine the role of endogenous ERp29 in regulation of ER stress, we applied ERp29 siRNA to downregulate the expression of ERp29. ARPE-19 cells were transfected with ERp29 siRNA or Ctrl siRNA for 48 hours, then treated with 320 μg/mL CSE for 6 or 24 hours. Western blot was used to determine target protein expression. Knockdown of ERp29 significantly decreased CSE-induced expression of GRP78 and caused a modest decrease in $p58^{IPK}$ expression (Fig. 4). Knockdown of ERp29 increased phosphorylation of eIF2α in nonstimulated cells, but not after CSE-treatment (Fig. 4), suggesting that a reduced ERp29 level may slow down protein synthesis by increasing eIF2α phosphorylation in resting cells. Downregulation of ERp29 also enhanced CSE-induced CHOP expression (Fig. 4), suggesting that ERp29-deficient cells may be vulner-

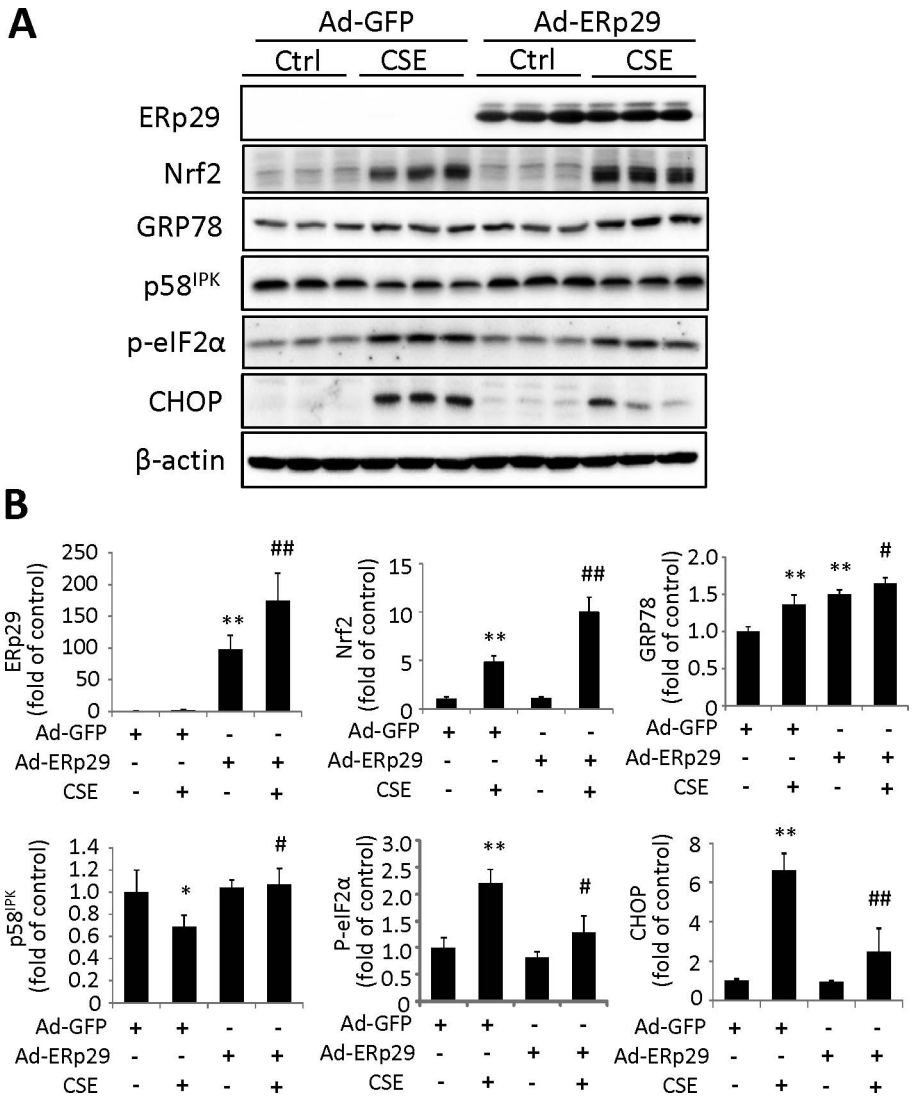

Figure 2. Overexpression of ERp29 alters the expression of ER stress factors and Nrf2 in HRPE cells. ARPE-19 cells were treated with Ad-ERp29 (20 multiplicity of infection, [MOI]) to induce ERp29 overexpression or Ad-GFP as control. The cells were then exposed to 320 μg/mL CSE for 6 hours (for measurement of p-eIF2α) or 24 hours (for measurement of other factors). (**A**) Representative Western blot images of ERp29, Nrf2, GRP78, $p58^{IPK}$, p-eIF2α, and CHOP. (**B**) Densitometry results of ERp29, Nrf2, GRP78, $p58^{IPK}$, p-eIF2α, and CHOP (normalized with β-actin) were analyzed. All data are expressed as the mean ± SD from three independent experiments. $^{*}P < 0.05$, $^{**}P < 0.01$ versus Ad-GFP; $\#P < 0.05$, $\#\#P < 0.01$ versus Ad-GFP + CSE.

able to ER stress-related apoptosis. In agreement with the result that Ad-ERp29 treatment increases Nrf2 expression, knockdown of ERp29 markedly reduced Nrf2 expression induced by CSE (Fig. 4).

To further determine if downregulation of ERp29 affects RPE cell survival, we examined apoptosis induced by CSE in ARPE-19 cells transfected with ERp29 or Ctrl siRNA. Using Western blot analysis, we noted a significant increase in the cleavage of PARP, a hallmark of apoptosis, induced by CSE in cells pretreated with ERp29 siRNA compared with cells pretreated with control siRNA (Fig. 5A). Interestingly, there was no further increase in caspase-3 activation in the ERp29 knockdown group (Fig. 5A). The TUNEL assay showed an increased number of apoptotic cells in the ERp29 knockdown group after exposure to CSE (Fig. 5B). This result was further confirmed by trypan blue staining, which showed more dead cells in the ERp29 knockdown group (Fig. 5C).

Erp29 Improves RPE Barrier Integrity and Protects Against CSE-Induced Tight Junction Damage

Endoplasmic reticulum protein 29 has been reported to regulate epithelial integrity in cancer cells.[14] To determine the role of ERp29 in RPE barrier integrity, we examined the expression of the tight junction protein, ZO-1, in ARPE-19 cells after overexpression or knockdown of ERp29. Overexpression of ERp29 significantly attenuated CSE-induced ZO-1 reduction, but did not alter the basal level of this protein (Fig. 6A). In contrast, knockdown of ERp29 reduced the baseline level of ZO-1 compared with control siRNA group (Fig. 6B). Cigarette smoke extract induced a similar extent of reduction in the ERp29 knockdown and control groups. To further ascertain if ERp29 had an impact on ZO-1 protein distribution and tight junction formation, we performed immunofluorescence staining of ZO-1 in ARPE-19 cells. Tight junction formation was evaluated and graded into the following four levels: "smooth";

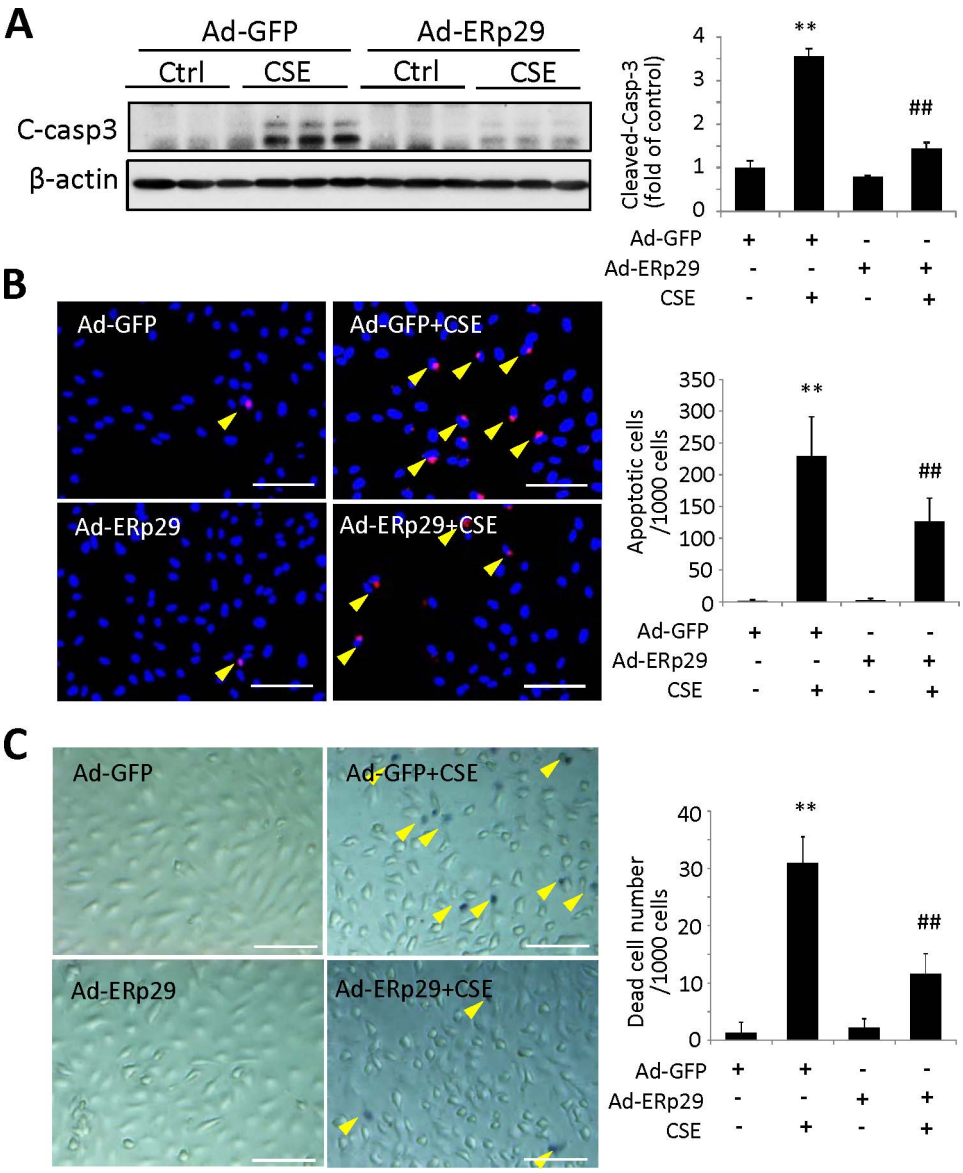

Figure 3. Overexpression of ERp29 protects HRPE cells from CSE-induced apoptosis and cell death. ARPE-19 cells were treated with Ad-ERp29 (20 MOI) to induce ERp29 overexpression or Ad-GFP as control, and then exposed to 320 μg/mL CSE for 24 hours. (**A**) Protein level of cleaved caspase-3 was determined by Western blot analysis. *Left*: Western blot images, *right*: densitometry results normalized with β-actin. (**B**) Apoptosis was examined by the TUNEL assay. *Left*: TUNEL assay images. *Scale bars*: 100 μm. *Right*: Quantification of TUNEL-positive cells. (**C**) Dead cells were detected using in situ trypan blue staining. *Left*: Images of trypan blue staining. *Scale bars*: 100 μm. *Right*: Quantification of trypan blue staining. All data are expressed as the mean ± SD from three independent experiments. $^{**}P < 0.01$ versus Ad-GFP; $^{\#\#}P < 0.01$ versus Ad-GFP + CSE.

"complete"; "broken"; and "disappeared." Overexpression of ERp29 significantly improved tight junction formation, as evidenced by smooth and or rough ZO-1 staining along cell borders (Fig. 6C). Overexpression of ERp29 also alleviated tight junction damage (discontinuous, disrupted, or absent ZO-1 staining on the cell surface) in ARPE-19 cells after CSE treatment for 6 (not shown) or 24 hours (Fig. 6C). In agreement with these changes, the TEER assay, which measures electrical resistance of the cell monolayer,[38] showed that CSE-induced time-dependent reduction in TEER was attenuated by Ad-ERp29 in ARPE-19 cells (Fig. 6D).

Furthermore, immunostaining using phalloidin indicated that CSE significantly reduced the expression of F-actin, which was partially prevented by pretreatment with Ad-ERp29 (Fig. 7A). Given the important role of F-actin, we speculate that the CSE-induced tight junction damage may be partly caused by the CSE induced F-actin damage. To address the issue of CSE-induced F-actin damage playing a more substantial role, we examined adherens junction (AJ) markers using immunostaining in ARPE-19 cells challenged with 160 μg/mL CSE for 24 hours. We found that CSE treatment altered distribution of AJ markers, pan-cadherin (Fig. 7B) and β-catenin (Fig. 7C) and substantially decreased ZO-1 staining (not shown), when compared with controls. For both markers we found islands of staining in the cytosol in many more CSE-treated cells than in controls, perhaps indicative of a damaged F-actin network. Furthermore, we found a decrease in consistent labeling of pan cadherin around the periphery of CSE-treated cells, with many cells displaying discontinuous labeling at apparent cell–cell contacts.

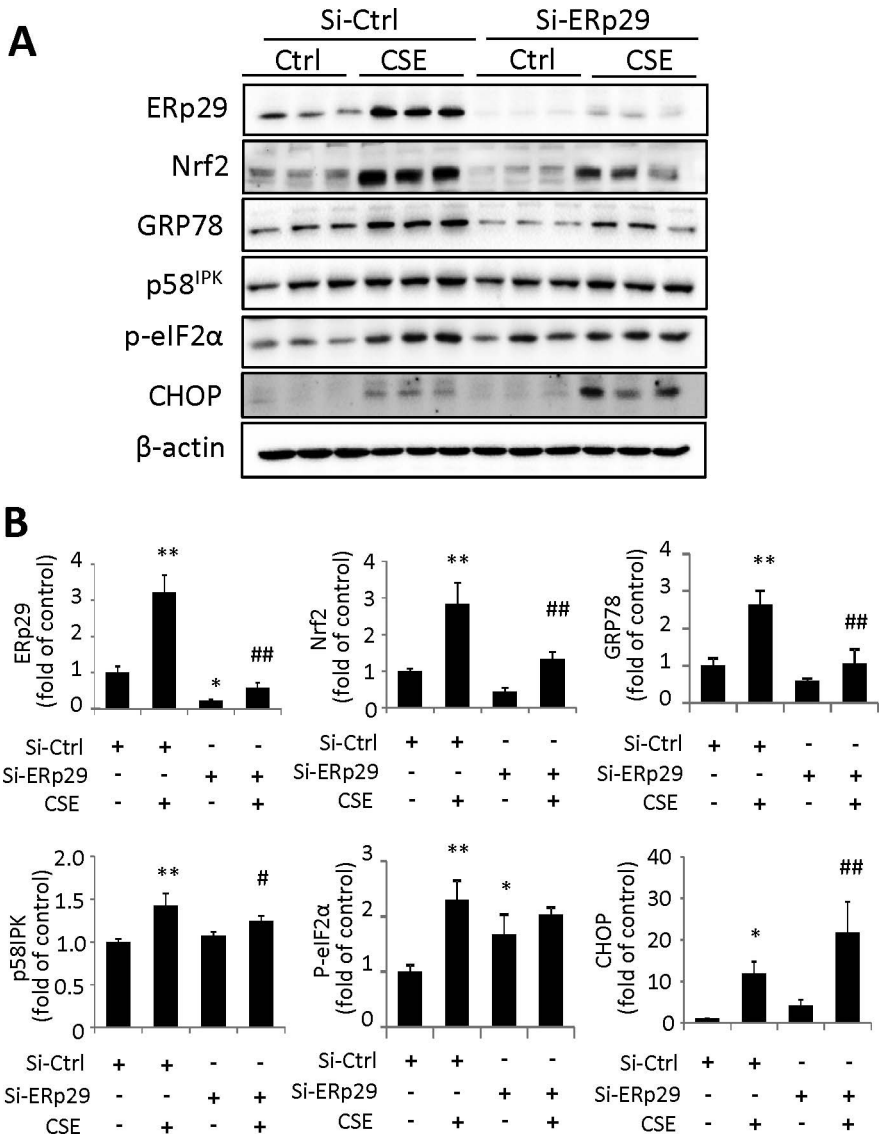

Figure 4. Knockdown of ERp29 reduces intracellular levels of ER chaperones and Nrf2 but increases CHOP in human RPE cells. ARPE-19 cells were transfected with siRNA targeting ERp29 (Si-ERp29) or Ctrl siRNA (Si-Ctrl), then treated with 320 μg/mL CSE for 6 hours (for measurement of p-eIF2α) or 24 hours (for measurement of other factors). (**A**) Protein levels of ERp29, Nrf2, GRP78, p58^{IPK}, p-eIF2α, and CHOP were determined by Western blot analysis. (**B**) Densitometry results of ERp29, Nrf2, GRP78, p58^{IPK}, p-eIF2α, and CHOP (normalized with β-actin) were analyzed. All data are expressed as the mean ± SD from three independent experiments. $^{*}P < 0.05$, $^{**}P < 0.01$ versus Si-Ctrl; $\#P < 0.05$, $\#\#P < 0.01$ versus. Si-Ctrl + CSE.

Discussion

The chaperone protein ERp29 is induced by a variety of cellular stressors,[2,39,40] but is reduced in the retina of AMD patients.[5,19] Using cultured RPE cells and mouse eyecup explants, we show that ERp29 was slightly upregulated by transient CSE (320 μg/mL for 6 hours) but more substantially (by 1.5-fold relative to controls) in response to longer CSE exposure (320 μg/mL for 24 hours). Likewise, short-term CSE treatment induces ER stress and increases expression of other ER chaperones such as GRP78 and p58^{IPK}[32]. These findings are, however, contradictory to the observation of decreased ERp29 level in human AMD. We speculate that this discrepancy may be related to the difference in the model system (i.e., acute stress condition induced by CSE versus chronic or even late-stage AMD where retinal damage is severe and the effects outweigh that of ER stress on ERp29 expression). To address this issue, we examined the ERp29 level in ARPE-19 cells after long-term treatment of CSE. Our results show that 3-week, but not 10-day, incubation with CSE reduced ERp29 expression, suggesting that chronic stress condition may impair the ER function by reducing the level of ER chaperones.

Our data suggest that ERp29 alleviates ER stress induced by CSE and protects RPE cells from apoptosis. In response to ER stress, the cell activates a set of signaling pathways known as the unfolded protein response (UPR), which coordinates multiple distinct programs to modulate protein synthesis, folding, and ER-associated degradation (ERAD).[41,42] Among the UPR pathways is the PKR-like endoplasmic reticulum kinase (PERK)–eIF2α–ATF4–CHOP branch. During the early stages of ER stress, activation of PERK phosphorylates eIF2α reducing the protein translation rate in the ER. In later stages, eIF2α phosphorylation activates the downstream gene CHOP, which may lead to apoptotic cell death.[41,43,44] Expression of ERp29 is closely related to that of PERK; ERp29 overexpression

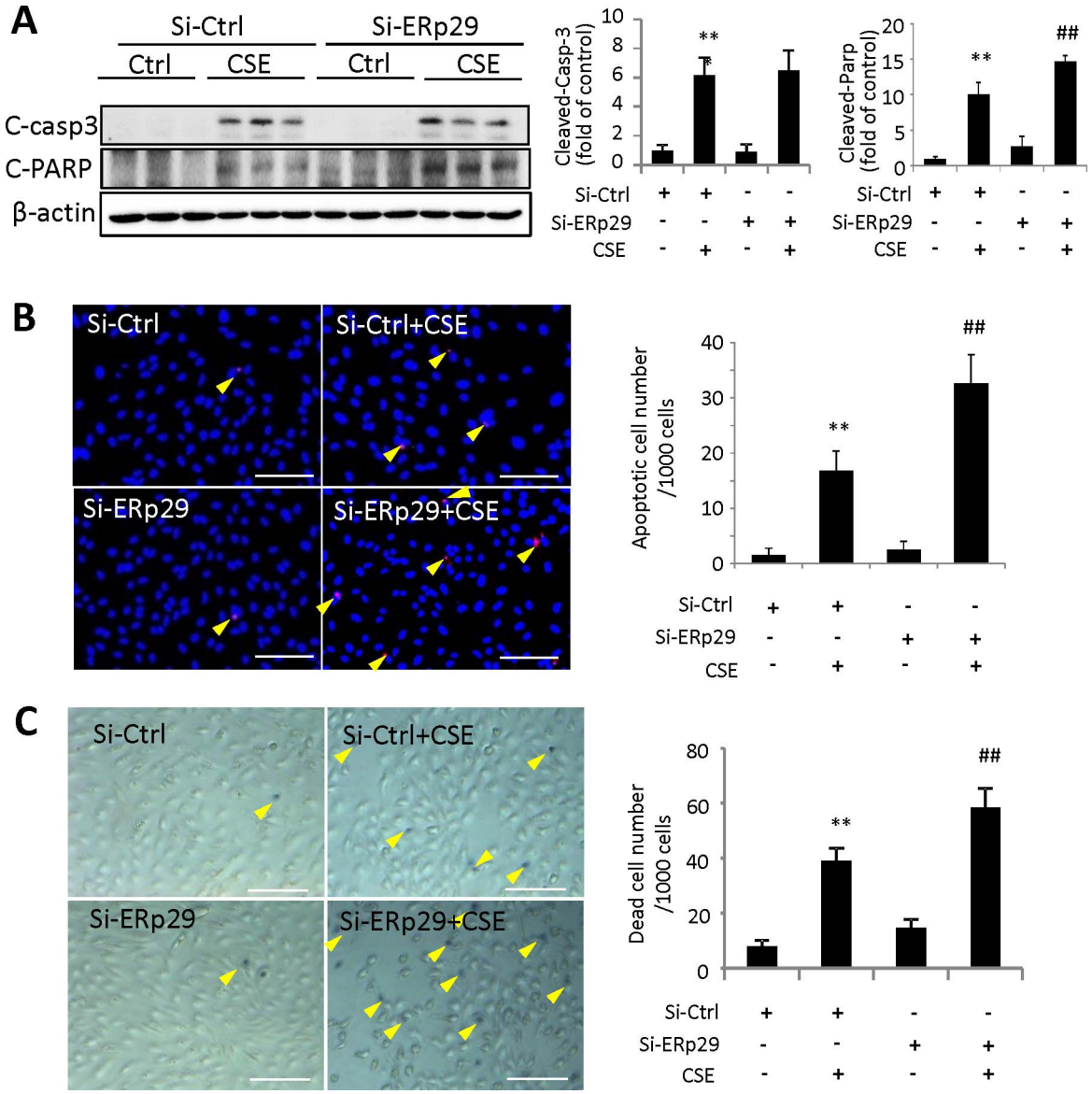

Figure 5. Knockdown of ERp29 exacerbates CSE-induced apoptosis and cell death in human RPE cells. ARPE-19 cells were transfected with siRNA targeting ERp29 (Si-ERp29) or Ctrl siRNA (Si-Ctrl), then treated with 320 μg/mL CSE for 24 hours. (**A**) Protein levels of cleaved caspase-3 and cleaved PARP were determined by Western blot analysis. *Right*: Western blot images. *Left*: Densitometry results normalized with β-actin. (**B**) Apoptosis of ARPE-19 cells was examined by the TUNEL assay. *Left*: TUNEL assay images. *Scale bars*: 100 μm. *Right*: Quantification of TUNEL-positive cells. (**C**) Dead cells were detected using trypan blue staining. *Left*: Images of trypan blue staining. *Scale bars*: 100 μm. *Right*: Quantification of trypan blue staining. All data are expressed as the mean ± SD from three independent experiments. $^{**}P < 0.01$ versus Si-Ctrl; $^{\#\#}P < 0.01$ versus Si-Ctrl + CSE.

enhanced total PERK levels, while suppression of ERp29 expression or inhibition its function by a dominant-negative mutant reduced the level of this protein.[40] In addition, ERp29 also increased phosphorylation of MAPK p38 (p-p38) and eIF2α phosphorylation.[9] Furthermore, overexpression of ERp29 increased expression of $p58^{IPK}$, a cochaperone for GRP78 that also functions as an inhibitor of PERK to suppress eIF2α phosphorylation.[45] Upregualtion of $p58^{IPK}$ may also suppress the activation of p-p38, thereby repressing eIF2α phosphorylation.[9] These regulations could be important mechanism for the feedback regulation of protein synthesis by ER chaperones.

In agreement with previous findings that ERp29 regulates other chaperone molecule expression, we observed that overexpression of ERp29 increased the levels of GRP78 and $p58^{IPK}$, while knockdown of ERp29 decreased that of $p58^{IPK}$ in RPE cells. Furthermore, enhancing ERp29 expression significantly reduced CSE-stimulated p-eIF2α and CHOP expression and protected RPE cells from apoptosis. In contrast, knockdown of ERp29 exacerbated CSE-triggered CHOP activation and apoptosis. This suggests that endogenous ERp29 is important for RPE cells to protect against CSE-induced ER stress and subsequent apoptosis. Additionally, we report a novel function of ERp29 in regulation of Nrf2, a bZip transcription factor that induces antioxidant responsive element (ARE)-regulated genes encoding phase II detoxification enzymes and antioxidant proteins, thereby protecting cells from oxidative damage. Overexpression of ERp29 enhanced, while knockdown of ERp29 reduced, CSE-stimulated Nrf2 upregulation; yet in both conditions the basal level of

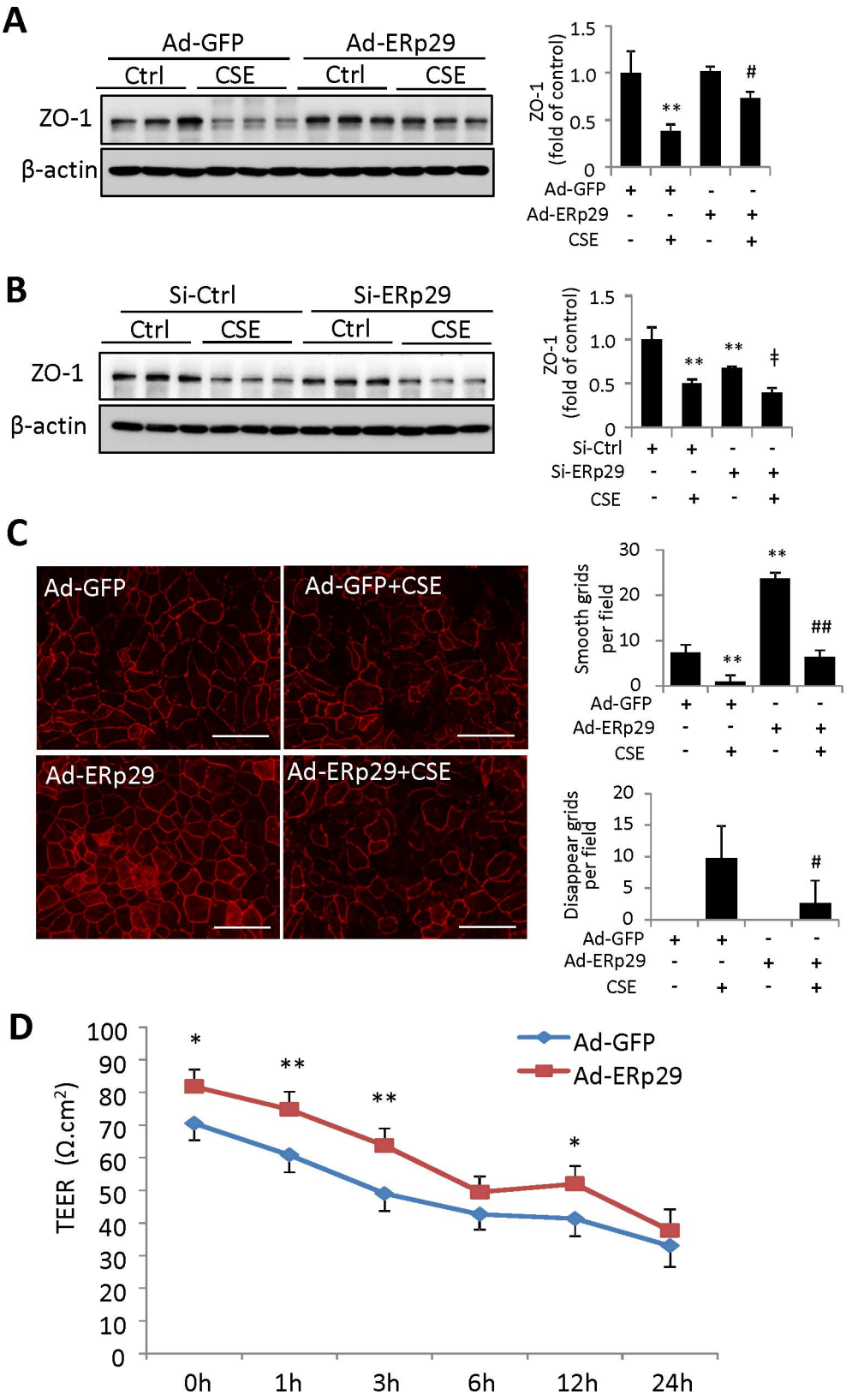

Figure 6. Endoplasmic reticulum protein 29 enhances tight junction protein ZO-1 formation and protected the tight junction from CSE damage in ARPE-19 cells. (**A**) ARPE-19 cells were treated with Ad-ERp29 (20 MOI) or Ad-GFP as control, and then exposed to 320 μg/mL CSE for 24 hours. Protein level of ZO-1 was examined by Western blot. *Left*: Western blot images. *Right*: Densitometry results of ZO-1 (normalized with β-actin). (**B**) ARPE-19 cells were transfected with siRNA targeting ERp29 (Si-ERp29) or Ctrl siRNA (Si-Ctrl), then treated with 320 μg/mL CSE for 24 hours. Protein level of ZO-1 was examined by Western blot. *Left*: Western blot images. *Right*: Densitometry results of ZO-1 (normalized with β-actin). (**C**) Immunofluorescence staining of ZO-1 in Ad-ERp29-transduced ARPE-19 cells after exposure to CSE (160 μg/mL) for 24 hours. *Left*: Immunofluorescence staining results of ZO-1. *Scale bars*: 100 μm. *Right*: Qualification of ZO-1 morphologic changes in "smooth" and

Investigative Ophthalmology & Visual Science

"disappeared" grades. (**D**) Transepithelial electrical resistance (TEER) of Ad-ERp29-transduced ARPE-19 cells at 0, 1, 3, 6, 12, and 24 hours after exposure to CSE (160 μg/mL). All data are expressed as the mean ± SD from three independent experiments. $^{*}P < 0.05$, $^{**}P < 0.01$ versus Ad-GFP; $\#P < 0.05$, $\#\#P < 0.01$ versus Ad-GFP + CSE.

Nrf2 did not seem to change by ERp29 manipulation. This suggests that ERp29 may regulate Nrf2 protein production, likely through regulation of molecules induced by ER stress and the UPR pathways; however, the exact mechanism remains elusive and is beyond the scope of this study.

A recent study revealed that intravitreal injection of CSE damages the mouse RPE tight junctions and potentially promotes EMT.[27] The RPE tight junctions are important in maintaining retinal homeostasis and regulate the flow of solutes from the fenestrated capillaries of the choroid to retinal photoreceptor cells.[46,47] The tight junction–associated protein ZO-1 is a ubiquitous cytoskeletal-associated protein belonging to the membrane associated guanylate kinase (MAGUK) family.[48] It provides a multidomain structure for protein complexes to assemble on the cytoplasmic surface of the plasma membrane and functionally couple transmembrane proteins to the cytoskeleton.[49] Moreover, the terminal of ZO-1 embeds into different functional areas of the tight junction and interacts with multiple membrane proteins to regulate interactions with the cytoskeleton.[49] We confirmed that CSE can effectively inhibit the expression of ZO-1, disrupt the morphology of tight junctions, reduce the TEER value, and diminish the cytoskeleton protein F-actin in cultured RPE cells. We also found that overexpression of ERp29 attenuated the CSE-induced reduction in ZO-1 level, while ERp29 knockdown decreased ZO-1 expression. Immunostaining and TEER assays showed that overexpression of ERp29 improved ZO-1 distribution and attenuated CSE-induced tight junction disruption or functional damage. Notably, we found that the changes in tight junctions (as measured by ZO-1 Western blotting and staining) may be understated due to cell to cell variability in ERp29 expression after adenoviral transduction (data not shown). These results suggest a protective effect of ERp29 on RPE barrier integrity, and also imply a potential role of ERp29 in reducing EMT and preventing the development of CNV, which will warrant future investigation.

Finally, our study verified that the CSE-induced structural and functional damage to tight junctions may be partially related to disruption of the F-actin cytoskeleton. The actin cytoskeleton is considered a critical regulator of tight junction

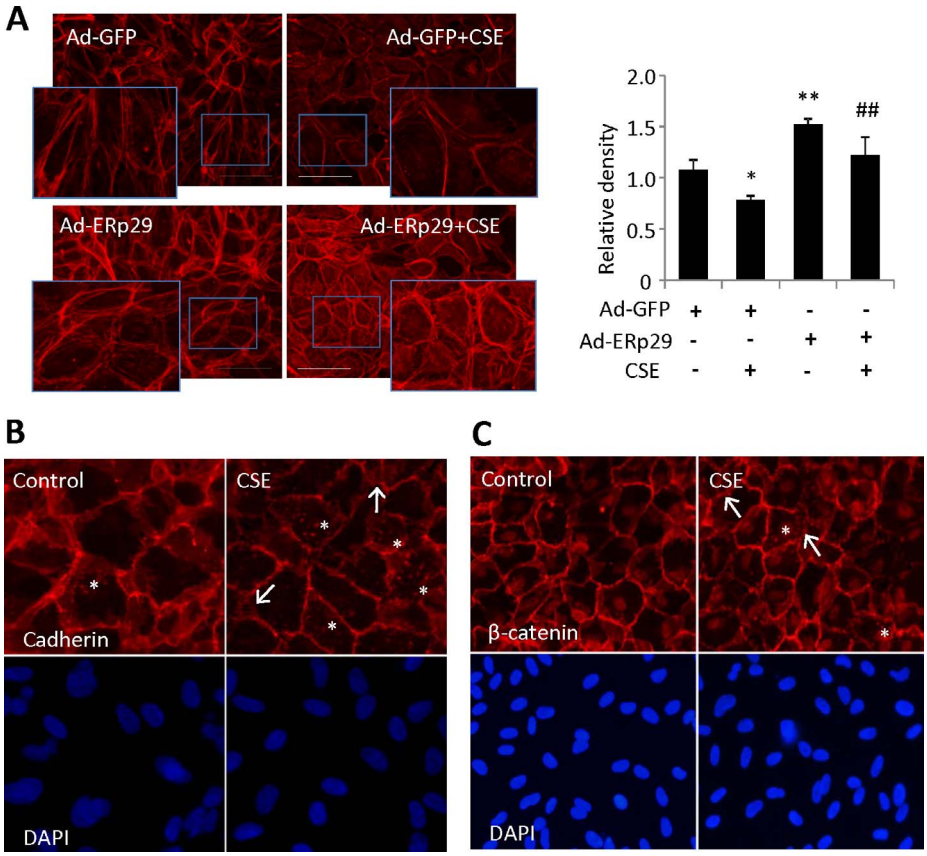

Figure 7. Overexpression of ERp29 enhanced F-actin expression in human RPE cells. (**A**) Expression and distribution of F-actin was detected by immunofluorescence staining in ARPE-19 cells challenged with CSE (160 μg/mL) for 24 hours. *Left*: Images of phalloidin (F-actin) staining. *Scale bars*: 100 μm. *Right*: Quantification of F-actin, as measured by relative density. Data are expressed as the mean ± SD from three independent experiments $^{*}P < 0.05$, $^{**}P < 0.01$ versus Ad-GFP; $\#P < 0.05$, $\#\#P < 0.01$ versus Ad-GFP + CSE. (**B**, **C**) ARPE-19 cells were treated with 160 μg/mL CSE for 24 hours and stained for adherens junction markers pan-cadherin and β-catenin. In control conditions, most cells have strong, continuous labeling of both markers around their entire periphery. (**B**) Cigarette smoke extract–treated cells reveal a reduced level of cadherin and the labeling is often discontinuous around the periphery of the cell. In contrast to control, many cells under CSE treatment have patches of cadherin present throughout the cell (*asterisks*). Strongly labeled fibrils between adjacent cells are also more prominent (*arrows*). (**C**) In CSE-treated cells, β-catenin labeling includes patches present throughout the cell (i.e., not limited to the periphery or nucleus as in control; *asterisks*) with strongly labeled fibrils between adjacent cells (*arrows*). DAPI labeling confirms a similar density of cells in each field.

Investigative Ophthalmology & Visual Science

assembly and many cytoplasmic constituents of tight junctions are directly or indirectly associated with F-actin.[50] In addition, F-actin is important for microvilli formation and participates in other types cell–cell and cell–matrix junctions such as adherens junctions. To determine a potential role of F-actin in CSE-induced RPE damage, we extended the experiments to include staining for adherens junction markers in ARPE-19 cells challenged with CSE. Our results show that CSE not only disrupted tight junction formation, but also altered F-actin and adherens junctions. Furthermore, overexpression of ERp29 upregulated F-actin expression in RPE cells and alleviated CSE-induced F-actin disruption. These results suggest that CSE alters F-actin and damages cell junctions, and enhanced F-actin expression may be one mechanism through which ERp29 protects the RPE against ER stress. However, the mechanisms by which CSE induces F-actin damage and the effects of ERp29 on protection of F-actin-related RPE structure and function remain elusive.

In summary, in the present study we demonstrate that ERp29 attenuates CSE-induced ER stress, reduces apoptosis, and mitigates the damage of tight junctions in RPE cells. Our findings indicate a protective role of ERp29 against cigarette smoke–related RPE injury, which is pertinent to the development of AMD. However, the mechanisms by which ERp29 regulates the prosurvival pathways such as Nrf2 and enhances the RPE barrier integrity, as well as the exact role of ERp29 in tight junction formation, remain to be investigated. Furthermore, animal studies using targeted deletion of ERp29 or overexpression of the protein are needed to establish the function of ERp29 in the RPE in vivo, and to provide more definitive information on the role of ERp29 in the development of AMD using relevant animal models.

Acknowledgments

The authors thank Todd McLaughlin for technical assistance in immunocytochemistry.

Supported in part by National Institutes of Health/National Eye Institute (Bethesda, MD, USA) Grants EY019949 and EY025061, by a grant from American Diabetes Association (Alexandria, VA, USA), and by an unrestricted grant to the Department of Ophthalmology, SUNY-Buffalo, from Research to Prevent Blindness (all to SXZ; New York, NY, USA).

Disclosure: **C. Huang**, None; **J.J. Wang**, None; **G. Jing**, None; **J. Li**, None; **C. Jin**, None; **Q. Yu**, None; **M.W. Falkowski**, None; **S.X. Zhang**, None

References

1. Demmer J, Zhou C, Hubbard MJ. Molecular cloning of erp29, a novel and widely expressed resident of the endoplasmic reticulum. *FEBS Lett*. 1997;402:145–150.
2. Mkrtchian S, Fang C, Hellman U, Ingelman-Sundberg M. A stress-inducible rat liver endoplasmic reticulum protein, erp29. *Eur J Biochem*. 1998;251:304–313.
3. Hubbard MJ, McHugh NJ. Human erp29: isolation, primary structural characterisation and two-dimensional gel mapping. *Electrophoresis*. 2000;21:3785–3796.
4. Chandra H, Gupta PK, Sharma K, et al. Proteome analysis of mouse macrophages treated with anthrax lethal toxin. *Biochim Biophys Acta*. 2005;1747:151–159.
5. Verma V, Sauer T, Chan CC, et al. Constancy of erp29 expression in cultured retinal pigment epithelial cells in the ccl2/cx3cr1 deficient mouse model of age-related macular degeneration. *Curr Eye Res*. 2008;33:701–707.
6. Seo S, Kwon YS, Yu K, et al. Naloxone induces endoplasmic reticulum stress in pc12 cells. *Mol Med Rep*. 2014;9:1395–1399.
7. Liepinsh E, Baryshev M, Sharipo A, Ingelman-Sundberg M, Otting G, Mkrtchian S. Thioredoxin fold as homodimerization module in the putative chaperone erp29: NMR structures of the domains and experimental model of the 51 kDa dimer. *Structure*. 2001;9:457–471.
8. Park S, You KH, Shong M, et al. Overexpression of Erp29 in the thyrocytes of FRTL-5 cells. *Mol Biol Rep*. 2005;32:7–13.
9. Gao D, Bambang IF, Putti TC, Lee YK, Richardson DR, Zhang D. Erp29 induces breast cancer cell growth arrest and survival through modulation of activation of p38 and upregulation of ER stress protein p58IPK. *Lab Invest*. 2012;92:200–213.
10. Hirsch I, Weiwad M, Prell E, Ferrari DM. ERp29 deficiency affects sensitivity to apoptosis via impairment of the ATF6-CHOP pathway of stress response. *Apoptosis*. 2014;19:801–815.
11. Sharma A, Sharma KK. Chemoprotective role of triphala against 1, 2-dimethylhydrazine dihydrochloride induced carcinogenic damage to mouse liver. *Indian J Clin Biochem*. 2011;26:290–295.
12. Zhang D, Putti TC. Over-expression of ERp29 attenuates doxorubicin-induced cell apoptosis through up-regulation of Hsp27 in breast cancer cells. *Exp Cell Res*. 2010;316:3522–3531.
13. Qi L, Wu P, Zhang X, et al. Inhibiting ERp29 expression enhances radiosensitivity in human nasopharyngeal carcinoma cell lines. *Med Oncol*. 2012;29:721–728.
14. Bambang IF, Lee YK, Richardson DR, Zhang D. Endoplasmic reticulum protein 29 regulates epithelial cell integrity during the mesenchymal-epithelial transition in breast cancer cells. *Oncogene*. 2013;32:1240–1251.
15. Klein R, Klein BE, Jensen SC, Meuer SM. The five-year incidence and progression of age-related maculopathy: the Beaver Dam Eye Study. *Ophthalmology*. 1997;104:7–21.
16. Fine SL, Berger JW, Maguire MG, Ho AC. Age-related macular degeneration. *N Engl J Med*. 2000;342:483–492.
17. Pieramici DJ, Bressler SB. Age-related macular degeneration and risk factors for the development of choroidal neovascularization in the fellow eye. *Curr Opin Ophthalmol*. 1998;9:38–46.
18. Hirasawa M, Noda K, Noda S, et al. Transcriptional factors associated with epithelial-mesenchymal transition in choroidal neovascularization. *Mol Vis*. 2011;17:1222–1230.
19. Tuo J, Bojanowski CM, Zhou M, et al. Murine ccl2/cx3cr1 deficiency results in retinal lesions mimicking human age-related macular degeneration. *Invest Ophthalmol Vis Sci*. 2007;48:3827–3836.
20. Age-Related Eye Disease Study Research Group. Risk factors associated with age-related macular degeneration. A case-control study in the age-related eye disease study: Age-Related Eye Disease Study Report Number 3. *Ophthalmology*. 2000;107:2224–2232.
21. Khan JC, Thurlby DA, Shahid H, et al. Genetic factors in AMDS. Smoking and age related macular degeneration: the number of pack years of cigarette smoking is a major determinant of risk for both geographic atrophy and choroidal neovascularisation. *Br J Ophthalmol*. 2006;90:75–80.
22. Tamakoshi A, Yuzawa M, Matsui M, Uyama M, Fujiwara NK, Ohno Y. Smoking and neovascular form of age related macular degeneration in late middle aged males: findings from a case-

control study in Japan. Research committee on chorioretinal degenerations. *Br J Ophthalmol*. 1997;81:901–904.

23. Wilson GA, Field AP, Wilson N. Smoke gets in your eyes: smoking and visual impairment in New Zealand. *N Z Med J*. 2001;114:471–474.
24. Fujihara M, Nagai N, Sussan TE, Biswal S, Handa JT. Chronic cigarette smoke causes oxidative damage and apoptosis to retinal pigmented epithelial cells in mice. *PLoS One*. 2008;3: e3119.
25. Espinosa-Heidmann DG, Suner IJ, Catanuto P, Hernandez EP, Marin-Castano ME, Cousins SW. Cigarette smoke-related oxidants and the development of sub-RPE deposits in an experimental animal model of dry AMD. *Invest Ophthalmol Vis Sci*. 2006;47:729–737.
26. Kunchithapautham K, Atkinson C, Rohrer B. Smoke exposure causes endoplasmic reticulum stress and lipid accumulation in retinal pigment epithelium through oxidative stress and complement activation. *J Bio Chem*. 2014;289:14534–14546.
27. Cano M, Wang L, Wan J, et al. Oxidative stress induces mitochondrial dysfunction and a protective unfolded protein response in RPE cells. *Free Radic Biol Med*. 2014;69:1–14.
28. Chen C, Cano M, Wang JJ, et al. Role of unfolded protein response dysregulation in oxidative injury of retinal pigment epithelial cells. *Antioxid Redox Signal*. 2014;20:2091–2106.
29. Csiszar A, Labinskyy N, Podlutsky A, et al. Vasoprotective effects of resveratrol and SIRT1: attenuation of cigarette smoke-induced oxidative stress and proinflammatory phenotypic alterations. *Am J Physiol Heart Circ Physiol*. 2008;294: H2721–H2735.
30. Huang C, Wang JJ, Ma JH, Jin C, Yu Q, Zhang SX. Activation of the UPR protects against cigarette smoke-induced RPE apoptosis through up-regulation of NRF2. *J Biol Chem*. 2015;290:5367–5380.
31. Rattner A, Toulabi L, Williams J, Yu H, Nathans J. The genomic response of the retinal pigment epithelium to light damage and retinal detachment. *J Neurosci*. 2008;28:9880–9889.
32. Huang C, Wang JJ, Ma JH, Jin C, Yu Q, Zhang SX. Activation of the UPR protects against cigarette smoke-induced RPE apoptosis through up-regulation of NRF2. *J Biol Chem*. 2015;290:5367–5380.
33. Zhong Y, Li J, Wang JJ, et al. X-box binding protein 1 is essential for the anti-oxidant defense and cell survival in the retinal pigment epithelium. *PLoS One*. 2012;7:e38616.
34. Li J, Wang JJ, Zhang SX. Preconditioning with endoplasmic reticulum stress mitigates retinal endothelial inflammation via activation of X-box binding protein 1. *J Biol Chem*. 2011;286: 4912–4921.
35. Chen C, Wang JJ, Li J, Yu Q, Zhang SX. Quinotrierixin inhibits proliferation of human retinal pigment epithelial cells. *Mol Vis*. 2013;19:39–46.
36. Chang YS, Wu CL, Tseng SH, Kuo PY, Tseng SY. Cytotoxicity of triamcinolone acetonide on human retinal pigment epithelial cells. *Invest Ophthalmol Vis Sci*. 2007;48:2792–2798.
37. Kim MH, Sonoi R, Yamada K, Inamori M, Kino-oka M. Analysis of locality of early-stage maturation in confluent state of human retinal pigment epithelial cells. *J Biosci Bioeng*. 2012; 113:778–781.
38. Ablonczy Z, Dahrouj M, Tang PH, et al. Human retinal pigment epithelium cells as functional models for the RPE in vivo. *Invest Ophthalmol Vis Sci*. 2011;52:8614–8620.
39. Bo Z, Yongping S, Fengchao W, Guoping A, Yongjiang W. Identification of differentially expressed proteins of gamma-ray irradiated rat intestinal epithelial IEC-6 cells by two-dimensional gel electrophoresis and matrix-assisted laser desorption/ ionisation-time of flight mass spectrometry. *Proteomics*. 2005; 5:426–432.
40. Farmaki E, Mkrtchian S, Papazian I, Papavassiliou AG, Kiaris H. ERp29 regulates response to doxorubicin by a perk-mediated mechanism. *Biochim Biophys Acta*. 2011;1813:1165–1171.
41. Walter P, Ron D. The unfolded protein response: from stress pathway to homeostatic regulation. *Science*. 2011;334:1081–1086.
42. Eizirik DL, Cardozo AK, Cnop M. The role for endoplasmic reticulum stress in diabetes mellitus. *Endocrine Rev*. 2008;29: 42–61.
43. Harding HP, Zhang Y, Bertolotti A, Zeng H, Ron D. PERK is essential for translational regulation and cell survival during the unfolded protein response. *Mol Cell*. 2000;5:897–904.
44. Zinszner H, Kuroda M, Wang X, et al. CHOP is implicated in programmed cell death in response to impaired function of the endoplasmic reticulum. *Genes Dev*. 1998;12:982–995.
45. Boriushkin E, Wang JJ, Zhang SX. Role of p58IPK in endoplasmic reticulum stress-associated apoptosis and inflammation. *J Ophthalmic Vis Res*. 2014;9:134–143.
46. Simo R, Villarroel M, Corraliza L, Hernandez C, Garcia-Ramirez M. The retinal pigment epithelium: something more than a constituent of the blood-retinal barrier–implications for the pathogenesis of diabetic retinopathy. *J Biomed Biotechnol*. 2010;2010:190724.
47. Rizzolo LJ. Development and role of tight junctions in the retinal pigment epithelium. *Int Rev Cytol*. 2007;258:195–234.
48. Herve JC, Derangeon M, Sarrouilhe D, Bourmeyster N. Influence of the scaffolding protein zonula occludens (zos) on membrane channels. *Biochim Biophys Acta*. 2014;1838: 595–604.
49. Van Itallie CM, Aponte A, Tietgens AJ, Gucek M, Fredriksson K, Anderson JM. The n and c termini of zo-1 are surrounded by distinct proteins and functional protein networks. *J Biol Chem*. 2013;288:13775–13788.
50. Fanning AS, Ma TY, Anderson JM. Isolation and functional characterization of the actin binding region in the tight junction protein zo-1. *FASEB J*. 2002;16:1835–1837.

Investigative Ophthalmology & Visual Science